Convective drying of green water lentil: kinetics analysis and modeling

A. Cabañas-Herrera[1*]; E. Moreno-Rodríguez[1]

[1]*Departamento de Ingeniería Química y Alimentos, Universidad de las Américas, Puebla. Santa Catarina Mártir, San Andrés Cholula, Puebla. C.P. 72810. México.*
**antonio.cabanasha@udlap.mx*

Abstract

The use of aquatic plants in wastewater treatment processes has been widely implemented in the XXI century given the plant's ability to reduce nitrogen and phosphorus levels in water. This paper studies the convective drying mechanism of green water lentil from an artificial wetland in UDLAP wastewater treatment system. The Taguchi methodology and variance analysis were used to analyze the variation of humidity with time to determine the most effective conditions for convective drying of green water lentil within the experiment design. The results of the experimental convective drying kinetics process suggest that the behavior of absolute humidity in time of the convective drying process of green water lentil can be modelled with a second-grade polynomial. The effective moisture diffusivity coefficients were determined as 2.84E-05cm^2/s for a 1000W resistance, 3.685cm^2/s for a 2000W resistance, and 5.427cm^2/s for a 4000W resistance for the convective drying process. Furthermore, these results are supported by convective drying models found in the literature for lentil drying under similar conditions. The results of this work might serve as the foundation for a potential energy analysis of green water lentil that allows the development of methods to minimize the impact of waste generated from wastewater treatment processes.

Keywords: *wastewater treatment*; *convective drying; green water lentil; kinetics analysis; modeling; Taguchi methodology;*

Introduction(Onwude et al., 2016)

The ever-growing implementation of wastewater treatment techniques and their innovation allows for a more sustainable exploitation of the water resources used for human activities. One of the main challenges in the treatment process is eutrophication, a phenomenon in which algae and phytoplankton undergo a sudden rise in growth due to the abundance of nutrients (Ferreira et al., 2020). The organic matter generated during eutrophication, along with the nitrogen (N) and phosphorus (P) that may have been discharged to the surface water, creates a much higher Chemical Oxygen Demand (COD) in the water (Al-Hashimi & Joda, 2010). When organisms like fish and other animal aquatic life die in these conditions, the bacteria which consume them have the potential to remove most of the oxygen available in the environment. Thus, degradation of the overall quality of a water body occurs (Al-Hashimi & Joda, 2010; Shammout & Zakaria, 2015).

A viable solution to avoid eutrophication is the implementation of ponds, natural or artificial wetlands, and lagoons where free-floating aquatic plants like the green water lentil are used to remove the excessive amount of P and N in water to render it appropriate for irrigation (Fertig, 2018). The different species of water lentil have an average 5.6 % dry mass, which includes a total protein content of 17-34 %, total fat content from 4-6 %, and a total starch content between 4 and 10 % (Appenroth et al., 2017). Several countries such as the USA, China, Jordan and Bangladesh have implemented the use of water lentil in full-scale wastewater treating systems (Al-Hashimi & Joda, 2010). In addition to nutrient removal, water lentil can inhibit the growth of algae and other aquatic plants that require sunlight by forming a thick layer at the surface that blocks the passage of light, keeping water cleaner (Shammout & Zakaria, 2015).

Mexican regulations NOM-001-SEMARNAT-1996, NOM-004-SEMARNAT-2002 apply to wastewater discharges in natural bodies of water and define maximum permissible limits of contaminants in the environment (CONAGUA, 1997). University of the Americas Puebla (UDLAP) in Mexico currently has a Wastewater Treatment Plant System (WWTPS) in its campus that incorporates an artificial wetland system (400 m^3, and 1-meter-deep). Figure 1 shows the overall treatment system that comprises granular activated sludge tanks (T1 & T2), a clarifier (T3) and a tertiary treatment (artificial wetland).

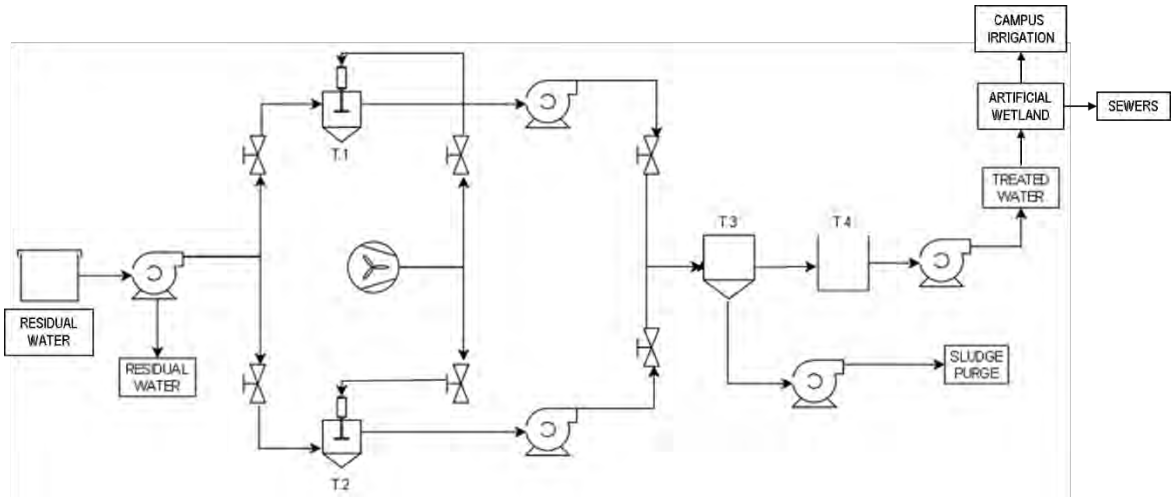

Figure 1. Process flow diagram of the water treatment process at UDLAP (Adapted from Aguilar, 2008).

Results were obtained following a Taguchi methodology developed considering controllable and noise variables to study their interaction in the drying process. In addition, parameters like activation energy, effective moisture diffusivity coefficient and effective moisture was calculated. Also, these results were compared with drying models found in the literature for lentil drying under similar conditions.

Methodology

Experiment setup

The wetland in UDLAP WWTS functions as a tertiary biological treatment consisting of an artificial open water body designed to treat water and remove residual suspended solids. The main vegetation present in UDLAP's wetland are tulle (*Typha domingensis*) and green water lentils, Figure 2.

Figure 2. Wetland located in UDLAP (Author)

Two kilograms of green water lentil were obtained from UDLAP's wetland in December 2019. During the sampling day, the weather conditions were a clear sky with abundant sun radiation, measuring conditions of 22°C dry bulb temperature (Ts), and 20.1°C wet bulb temperature (Tw). The specific volume of air at these conditions were 0.856 m^3/kg DA ($\bar{V}$), with an 85% average humidity (φ), 14.1 g/kg DA absolute humidity (h), and 58 kJ/kg enthalpy. All samples were stored in a plastic container at a steady temperature of 21±1°C for the duration of the experiment. In the following days when the experiment took place, the weather conditions showed some variability in Ts and Tw. For instance, in the days when the experiment was carried out, weather conditions were cold, humid mornings with high sun radiation, warmer temperatures and drier air around noon, and warm evenings. The drying process was carried out using a convection dryer with four electric resistances AE-61 type, of 1000 W each, a triphasic helical fan, digital balance, three trays, panel control, and humidity and temperature sensors at the inlet and outlet. The schematic diagram of the dryer used in the experiments is shown in Figure 3.

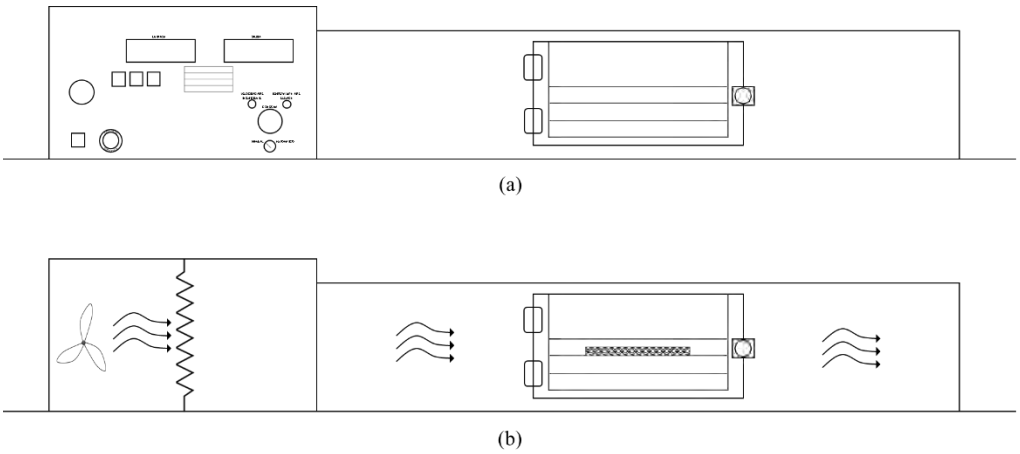

Figure 3. Schematic of convective drying equipment: a) Frontal view, b) Air flow direction (Author).

The lentil samples were prepared in a rectangle shape with the dimensions as shown in Figure 4a-c, and placed in the drier trays as shown in Figure 4d. During the drying process, the sample was weighted every five minutes using a digital balance with ±0.1 g accuracy.

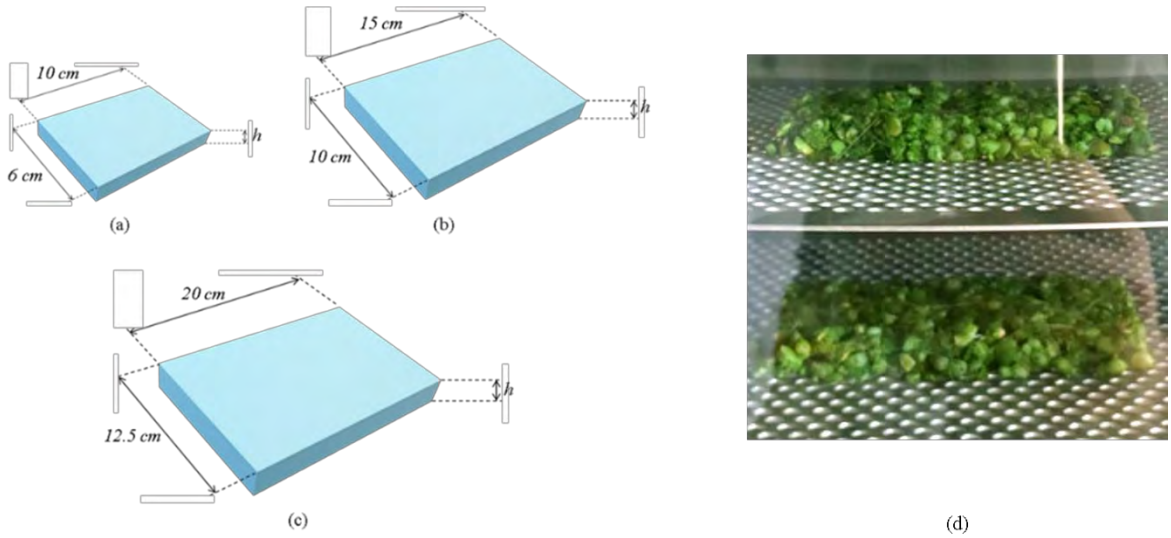

Figure 4. Transference area shapes and dimensions sample sizes: (a) low, (b) medium, (c) high,; (d) Exampe of sample distribution in the drying trays (Author).

Process analysis

Mathematical modeling of the drying rate

The mass humidity ($\mathcal{M}$) and the average mass humidity ($\bar{\mathcal{M}}$) of each sample were determined using Equations (1) and (2), where m_T is the total mass of the wet solid, m_D is the mass as a function of moisture content, and n denotes the interval time. Furthermore, the drying rate flux (R) was determined using Equation (3), where $\mathcal{A}$ is the interfacial area exposed in a specific time (dt). All measures were considered on dry basis.

$$\mathcal{M}_n = \frac{m_{Tn} - m_{Dn}}{m_{Dn}} \quad (1)$$

$$\overline{\mathcal{M}}_n = \frac{\mathcal{M}_n + \mathcal{M}_{n+1}}{2} \quad (2)$$

$$\mathrm{R_n} = -\frac{\mathrm{m_{Dn}}}{\mathcal{A}} \frac{\mathrm{d}\overline{\mathcal{M}}}{\mathrm{dt}} \quad (3)$$

The consideration of assumptions was necessary for the modeling stage. The assumptions for thin layer drying models considered were (Çalışkan Koç & Çabuk, 2019; Onwude et al., 2016; Seader & Henley, 2005):

- Moisture was initially uniformly distributed throughout the mass of the product.
- Layers of material were fully exposed to a uniform airstream during drying.
- The surface moisture content of the sample instantaneously reached equilibrium with the condition of the surroundings.
- Resistance to mass transfer at the liquid-gas interface was negligible.
- It was assumed that the temperature distribution of a thin-layer material is uniform.
- The shrinkage and case hardening were negligible.

Variables analysis

Taguchi proposed an approach to solving the Robust Parameter Design (RPD) problem based on designed experiments and some novel methods for analysis of the resulting data (Montgomery, 2008). The RPD approach implies the definition of optimal levels for the controllable variables of a process and defines system as the ensemble of products and processes (Robinson et al., 2004). Taguchi methodology is widely used in the industry and has been proven can optimize parameters and improve process performance of systems using a minimum number of experiments (Liu et al., 2019; Mirzaee et al., 2009; Mohammadi et al., 2019; özdemir, 2020; Rao et al., 2004; Tun & Juchelková, 2019). An important aspect of Taguchi methodology was the notion that certain types of variables cause variability in important system response variables, and that measures are sensitive to noise factors like external noise, manufacturing variations and product deterioration (Montgomery, 2008).

The application of the Taguchi RPD is considered since controllable and uncontrollable noise variables have been identified in the convective drying process. Weather conditions are not entirely predictable, and not constant. Therefore, among other variables (figure 5), six noise variables (NV) were identified as capable to affect the water green lentils drying process: time of the day, dry temperature, wet bulb temperature, balance precision, and equipment stabilization time. Table 1 describes the relation between the identified six input NV and the convective drying process. From these six input NV, Ts and Tw were selected for the Taguchi RPD analysis, since these conditions are essential for the calculation of average humidity, which was considered for the Taguchi RPD methodology.

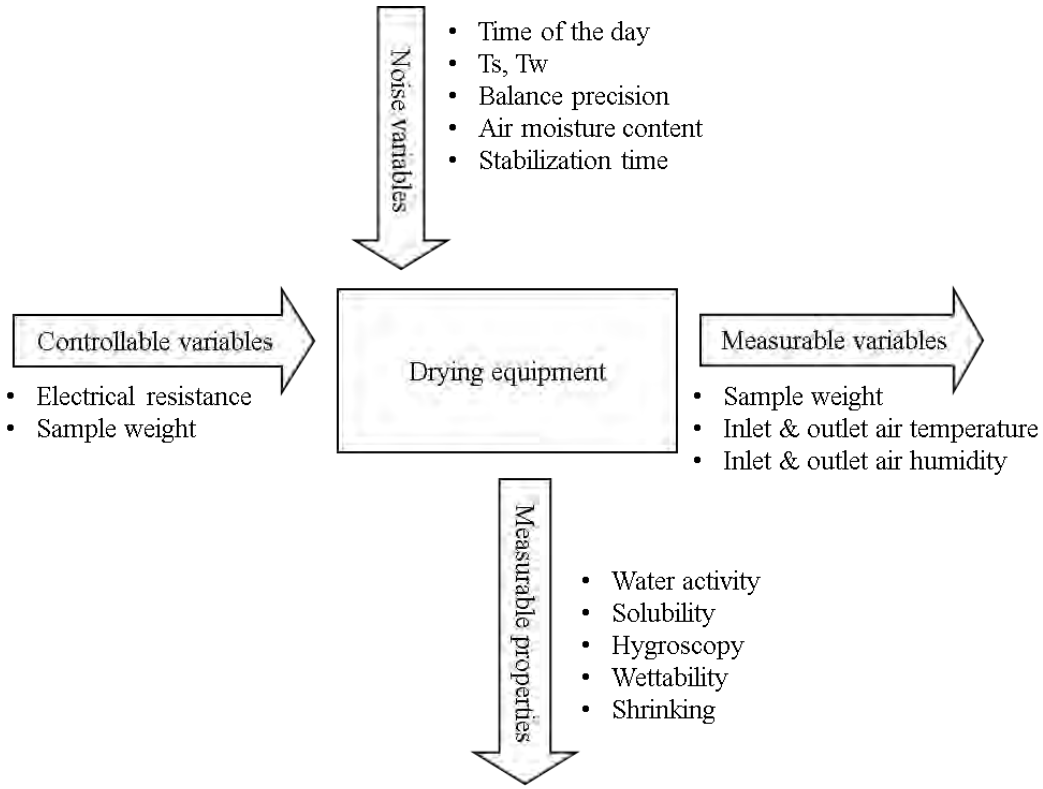

Figure 5. Variables, classified by type, involved in the drying process (Author).

Table 1. Description of the Noise Variables in the drying process.

NV	Description	Range of values			
1	Time of the day	Early morning	Late morning	Early evening	Late evening
2	Ts, °C	17-18.9	19-20.9	21-22.9	23-25
3	Tw, °C	13-14.9	15-16.9	17-18.9	19-21
4	Balance precision, g	±0.1			
5	Stabilization time, min	25			

Table 2 presents the L9 (3^2) Taguchi designed experiment used in this study, where two controllable factors (A, electrical resistance and B, sample weight) were stablished, each one at three levels. Ts and Tw were selected as a noise factors, producing a Taguchi experimental design of three-level fractional factorial pictured in Figure 3. The orthogonal array for this design is presented in Table 3.

Table 2. Key controllable factors and levels (Author).

Label	Factor	Level	Measure
A	Electrical resistance	1	1000 W
		2	2000 W
		3	4000 W
B	Sample weight	1	20g
		2	50g
		3	80g

Table 3 Taguchi's L9 orthogonal array for the drying experiments (Author).

Test	Factor A	Factor B
1	1	1
2	2	1
3	3	1
4	1	2
5	2	2
6	3	2
7	1	3
8	2	3
9	3	3

The Signal to Noise Ratio (SNR) response measures how the response varies relative to the nominal or target value under different conditions (Minitab, 2020). Table 4 shows some examples where the SNR models have been implemented to evaluate variable response, according to the SNR expressions of Minitab. In the analyses performed in this paper, larger-is-better SNR response was used to carry out the Taguchi analysis to maximize the measurable response of the selected variables under different conditions.

Table 4. Signal to noise ratios formulas (Adapted from Minitab, 2020).

Signal to noise ratio	Goal	Signal to noise ratio formulas	Examples
Larger is better	Maximize the response	$S/N = -10\ Log\left\{\sum(1/Y^2)/n\right\}$	An parameter for optimization was defined to investigate the influence of different control parameters on heat transfer and fluid flow characteristics (Mohammadi et al., 2019).
Nominal is best	Target the response and you want to base the signal to noise ratio on standard deviations only	$S/N = -10\ Log\{\sigma^2\}$	A relation between the uniformity measure U, and Taguchi's SNR for a Nominal-is-best- quality is studied with focus in a deposition process, using SNR for deposition thickness (Jung & Yum, 2011).
Nominal is best (default)	Target the response and you want to base the signal to noise ratio on means and standard deviations	$S/N = 10\ Log\{\bar{Y}^2/\sigma^2\}$ The adjusted formula is: $S/N = 10\ Log\{(\bar{Y}^2 - s^2/n)/s^2\}$	The results of threshold voltage in a 32nm PMOS transistor were analyzed and processed with the Taguchi Method to get the optimal design (Elgomati et al., 2012).
Smaller is better	Minimize the response	$S/N = -10\ Log\left\{\left(\sum Y^2\right)/n\right\}$	A hybrid method implementing principal component analysis, Taguchi's signal-to-noise ratio, and the normal boundary intersection was developed for the multiobjective optimization of 12L14 free machining steel turning process (Costa et al., 2016).

Results and discussion

Psychrometric analysis

Psychrometric charts are used to describe and quantify the drying processes, in particular the drying of a wet solid (water green lentil) by evaporation of the solid water content into the atmosphere (Seader & Henley, 2005) as depicted in Figure 6. In Figure 6 point A is the condition of the inlet air after heating; point B is the condition of liquid-gas interface of the water green lentil in the drier assuming thermodynamic equilibrium; and point C is the conditions air exit. The process pathway A-B is developed with a constant humidity, while pathway B-C shows an increase in relative humidity along the Tw axis, assuming an adiabatic humidification.

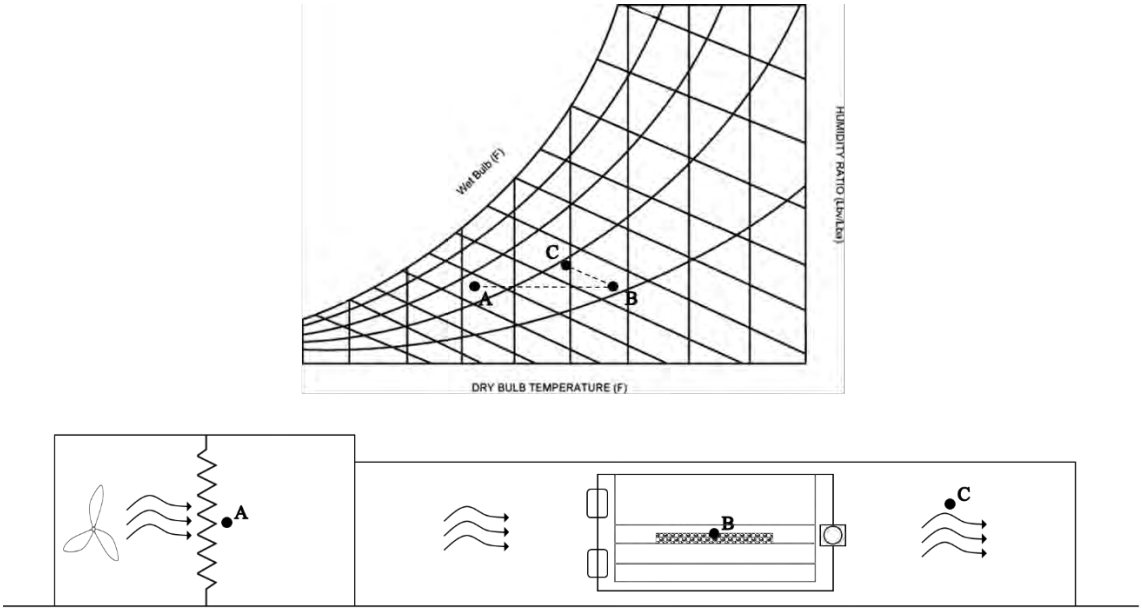

Figure 6. Process path description in (a) Psychometric chart, and (b) Schematic convective drying equipment.

Remarkably, as explained in the section Variables analysis, variable atmospheric conditions affect the measurable control variables at points A, B and C. Table 5 shows the psychrometric analysis performed on the convective drying process path. Analogically, the starting, critic, and final points refer to the moments in time when the test started, showed critic dehumidifying behavior, and finished, respectively. To perform the psychrometric analysis, a point was located in the psychrometric chart from Ts and Tw, and the rest of the thermodynamic conditions were measured from the graph at this point.

Note that, the conditions in the inlet, point A, are constant in time, since the atmospheric air coming into the drying equipment in this point was assumed unchanging in composition and conditions for the duration of the experiment. The consideration of the system behavior and thermodynamic characteristics allows a comprehensive understanding of the drying mechanism.

Table 5. Example of results of the psychrometric analysis performed on Test 8. Sample results table. Starting, critic, and final points are the three stages defined of the drying process (Author).

Variable	Starting point			Critic point			Final point		
	A	B	C	A	B	C	A	B	C
Ts, °C	21.8	32.8	31.8	21.8	32.3	31.1	21.8	31.7	30.4
Tw, °C	18.7	22	22	18.7	21.9	21.9	18.7	21.7	21.8

$\hat{v}$, m^3/kg DA*	0.852	0.883	0.881	0.852	0.882	0.879	0.852	0.880	0.878
φ, %	76	40	44	76	41	46	76	43	48
h, gr. W/kg DA*	12.4	12.3	12.7	12.4	12.3	12.8	12.4	12.3	12.9
$H_{measured}$, kJ/kg	53	64.9	65	53	64	64	53	63.5	64
H_{real}, kJ/kg	52.91	64.48	64.61	52.91	63.59	63.64	52.91	63.11	63.67

*DA, Dry Air

Effective moisture diffusivity and activation energy

The effective moisture diffusivity was determined following the moisture ratio (MR) methodology. The MR of the lentil seeds was calculated with Eq. (4), where $\mathcal{M}_0$, $\mathcal{M}_E$ and $\mathcal{M}_n$ represent moisture content (kg Water/kg Dry Lentil) at initial, equilibrium and in certain time, respectively.

$$MR = \frac{\mathcal{M}_n - \mathcal{M}_E}{\mathcal{M}_0 - \mathcal{M}_E} \quad (4)$$

The effective diffusion coefficient D_{eff}, Equation (5) was calculated considering Fick's second law of diffusion) and using two approaches: the first approach calculates D_{eff} defining k_0, Equation (6)as the slope of the plot *Ln (MR)* vs time. The Chi square error (X^2) was computed to evaluate the lineal model. The second approach uses an optimization technique to determine the value of D_{eff} that minimizes the sum of the residual squares X^2: The values of MR and D_{eff} for every interval were determined from Equations (5) and (7), respectively. Then, the optimum value of k_0 was obtained using Excel® Solver function, with the condition of yielding the lowest possible X^2 Error. Finally, an effective diffusion coefficient for each test was calculated from Equation (5).

$$MR = \frac{8}{\pi^2} \exp\left(-\frac{\pi^2 D_{eff}\, t}{4L^2}\right) \quad (5)$$

$$k_0 = \frac{\pi^2 D_{eff}}{4L^2} \quad (6)$$

where t stands for time, L is the sample´s thickness.

$$f(D_{eff}) = \sum_{i=1}^{n} \left(MR_i - MR_{exp}\right)^2 \quad (7)$$

Activation energy (E_a) was calculated using the Arrhenius Equation as function of the drying air temperature (T_a).

$$D_{eff} = D_0\, Exp\left(-\frac{E_a}{R\, Ta}\right) \quad (8)$$

Where D_0 is the pre-exponential factor (m^2/s); T_a (K); E_a is the energy of activation (J/mol); R is the constant of gas (8.3143 J/mol K). In order to calculate E_a, Equation (8) was linearized as follows:

$$\ln(D_{eff}) = Ln(D_0) - \frac{E_a}{R\, Ta} \quad (9)$$

Statistical analysis

ANOVA variance analysis

The experimental data obtained during the test was analyzed using analysis of variance (ANOVA), and a regression equation model using MiniTab Statistical Software v. 17. To carry out this task, the analyses were performed with a 95% confidence interval and a data normalization using a Box-Cox methodology. The ANOVA consisted on evaluate the resistance levels versus the sample weight to identify the behavior of average humidity and drying velocity.

It was observed that all P-Values are below α=0.05. Moreover, all P-values yielded α=0 for the change in average humidity as a response to sample weight levels and test runtime. Thus, it can be concluded that the average humidity in response to Variable Weight Sample (VWS) and time, showed a predictable behavior along the experiment, Table 6.

Table 6. Results of the ANOVA variance analysis (Author).

Resistance level	Response to	Degrees of freedom	
		Average humidity	Drying velocity
1	VWS	2	2
	Time	24	24
2	VWS	2	2
	Time	24	24
3	VWS	2	2
	Time	24	24

A benchmarking analysis was performed to determine the sigma capability (Cp_k) of the process as well as observing the deviations of results from the average model of each resistance level. This analysis was carried out by resistance level, and portrays a graphic behavior of the drying system, particularly of absolute humidity changes in time.

Figure 7 shows the general behavior of the drying process during which the dry base humidity decreases in time. See in Fig.7 a regression line (red) describing the general experiment behavior in each resistance level, while the three trajectories (dotted blue) describe the specific behavior of a run in that resistance level. Also note that in the lowest resistance level, a stable humidity is reached only at the end of the test, while in the medium level equilibrium was reached around minute 100, and in the highest resistance level equilibrium occurs around minute 70. This is expected since higher temperatures allow a faster rate of drying and moisture diffusion from the wet solid into the surrounding air.

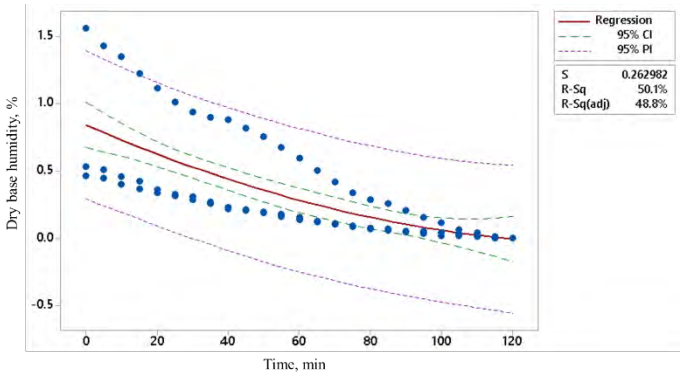

(a)

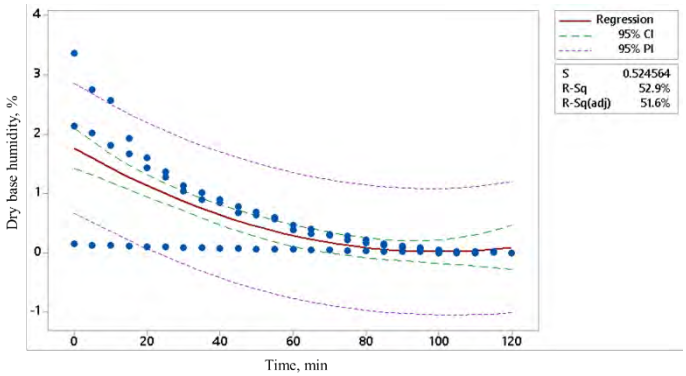

(b)

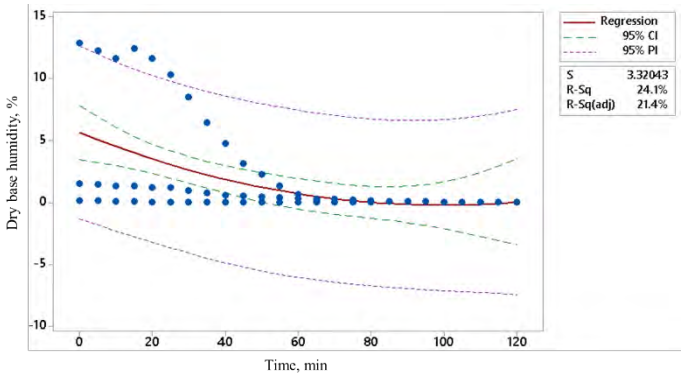

(c)

Figure 7. Benchmarking showing stabilization times for dry base humidity in response to (a) low, (b) medium, and (c) high resistance.

Regression analysis

A non-linear regression dynamic analysis of the mass humidity content was done for experimental data. During the fitting, several models were tested using the operation trend analysis in Excel®. Sum Square Error (SSE) and coefficient of determination (R^2) were also calculated n Table 8. The best drying model, Equation (10), was selected based on the lowest value of SSE, and X^2 and highest value of R^2. It is important to mention that test 6 on table 7, was not considered for the fitting of a regression equation model, since the humidity results of this test significantly deviated from the general behavior of the experiment. Nevertheless, the coefficient of determination was 0.9974, which suggested Test 6 does follow a behavior similar to the one described by Eq. 10.

Equation (10) represents the polynomial models used in the regression analysis described in Table 7. Where y is the dry base mass humidity response calculated by the regression model; a, b, and c are the regression coefficients for the polynomial equation; and t represents the drying time. Table 7 shows the coefficients of the regression models grouped by resistance level.

$$y = a\,t^2 + b\,t + c \qquad (10)$$

Table 7. Coefficients of the second-grade polynomial equation obtained for each resistance level in the regression models.

Test	T_a, °C	Resistance level	Model's coefficients			R^2
			a	b	c	
1	32.016	1	0.000037	-0.0114	0.8122	0.995
4	42.678					0.9719
7	55.619					0.9453
2	31.868	2	0.000201	-0.0339	1.6619	0.9968
5	33.392					0.9992
8	42.871					0.9500
3	29.704	3	0.000070	-0.0168	0.8686	0.9996
6	41.780					0.9974
9	44.060					0.9876

The SSE error was calculated evaluating the ability of each test's model to replicate the experimental results, as well as the ability of each group's model to replicate the same experimental results (See Table 8).

Table 8. Error Sum of Squares obtained in the regression models (Author).

Test	SSE Error	
	Model	Average in resistance level
1	0.03004	3.087
2	2.25264	11.532
3	0.00403	2.688
4	0.02270	0.657
5	0.71875	7.794
7	0.01243	0.852
8	0.00011	8.546
9	0.94323	3.3615

Table 9 presents a comparison between the models obtained in this paper and the model proposed by Işik et al., 2011 and Tang & Sokhansanj, 2007.
Although Isik et al. (2011) and this paper's experiments were not carried out under the same resistance values, it was possible to observe that the trend of Isik et al (2011) model of a reduction in the magnitude of the coefficients as the resistance value increases, is also present in this paper's models.

Table 9.Comparison of model coefficient between the current research and Işik et al., 2011 ;(Taşkin & İzlı, 2019)

Model	Equation	Model's coefficients

		300 W	400 W	700 W	800W	1000W	2000W	4000W
Taskin & Izli, 2019	$y = 1 + at + bt^2$				a= -0.00022 b= -0.00001			
Isik et al, 2011	$y = a + bt^2 + ct$	a=1.035 b=-1.69E-03 c=-0.00041	a=1.0253 b=-2.79E-03 c=-0.0005	a=1.0285 b=-9.11E0-2 c=-0.00056	a= 1.03705 b= -9.36E-02 c= -0.007			
This paper	$y = a + bt^2 + c$					a= 0.8122 b= -0.0114 a= 0.000037	a= 1.6619 b= -0.0339 a= 0.000201	a= 0.8686 b= -0.0168 a= 0.00007

Determination of the effective moisture diffusivity

The average humidity results were analyzed using the moisture ratio to determine the effective moisture diffusivity, Equations (4) and (5). Excel® Solver was used to determine the coefficient k_0 in the condition of yielding the lowest possible X^2 Error. Table 10 shows the values obtained for the moisture diffusivity and the X^2 Error, considering that the molecular diffusion coefficient of a certain chemical species through another depends on temperature and pressure conditions, and molecular forces like mass, volume, and intermolecular forces within the studied system (Murphy, 2015). In this work, the effective moisture diffusivity was determined based on the moisture ratio, which is in time defined by the humidity conditions measured at various moments in the experiment. Therefore, the obtained values for the moisture diffusivity coefficient are related with temperature and mass changes occurring during the drying process.

Table 10. Moisture diffusivity and Error values for the moisture ratio analysis.

Test	Resistance level	Sample weight level	Effective moisture diffusivity, cm^2/s	X^2 Error
1	1	1	2.543E-05	0.0133
2	2	1	5.017E-05	0.0045
3	3	1	9.357E-05	0.0064
4	1	2	3.081E-05	0.0085
5	2	2	3.564E-05	0.0102
6	3	2	3.714E-05	0.0476
7	1	3	2.913E-05	0.0115
8	2	3	2.473E-05	0.0123
9	3	3	3.209E-05	0.0183

Conclusions

The analysis of the effective moisture diffusivity coefficient was confirmed to be influenced by the system's conditions of temperature and pressure, among other molecular properties. In particular, since the drying process implies a change of mass and volume of the solid in time, this process therefore involves a mass transfer process in which intermolecular interactions are

present in the form of phase change, thus making it vulnerable to changes in atmospheric conditions. The kinetic drying process present in this paper, and in Isik et al (2011) at different resistance levels, shows similar trend polynomials coefficients, indicating that it is possible to predict the behavior of green lentil water. Also, the similitude between the two models supports the idea that the convective drying of water lentil can be modeled after a second-grade polynomial equation. From the psychrometric analyses, it is possible to conclude by observing the process path that before reaching the phase-change threshold, the system shows changes only in temperature and not in humidity, and subsequently, during the dehumidification, the system shows an adiabatic behavior under constant wet bulb temperature. The variance analysis showed a direct relation between the average moisture content in the sample and both the sample's weight and the time of the experiment. In fact, both the variance and benchmarking analyses support the close relation between sample weight and time in this convective drying process.

Future work could potentially focus on the improvement of the wetland in UDLAP Campus, particularly in the study of a more adequate aquatic species that enhances the flocculation mechanism carried out in the wetland. The replacement of green water lentil by red water lentil seems promising from a waste management and resource usage point of view, since literature reports that the higher levels of protein, amylose, and calcium improves coagulation and flocculation processes, which paired with a growth control could result in the reduction of both raw material needed and waste generation.

References

Aguilar, H. B. (2008). *Reactivación del sistema de tratamiento biológico SBR para la*. University of the Americas Puebla.

Al-Hashimi, M. A., & Joda, R. A. (2010). Treatment of Domestic Wastewater Using Duckweed Plant. *Journal of King Saud University - Engineering Sciences*, *22*(1), 11–18. https://doi.org/10.1016/S1018-3639(18)30505-1

Appenroth, K. J., Sree, K. S., Böhm, V., Hammann, S., Vetter, W., Leiterer, M., & Jahreis, G. (2017). Nutritional value of duckweeds (Lemnaceae) as human food. *Food Chemistry*, *217*, 266–273. https://doi.org/10.1016/j.foodchem.2016.08.116

Çalışkan Koç, G., & Çabuk, B. (2019). The effect of different microwave powers on the drying kinetics and powder properties of foam-mat dried egg white powder. *Gida / the Journal of Food*, *44*(2), 328–339. https://doi.org/10.15237/gida.gd18126

CONAGUA. (1997). *Normas Oficiales Mexicanas NOM-001-SEMARNAT-1996 NOM-002-SEMARNAT-1996 NOM-003-SEMARNAT-1997*. 65.

Costa, D. M. D., Paula, T. I., Silva, P. A. P., & Paiva, A. P. (2016). Normal boundary intersection method based on principal components and Taguchi's signal-to-noise ratio applied to the multiobjective optimization of 12L14 free machining steel turning process. *International Journal of Advanced Manufacturing Technology*, *87*(1–4), 825–834. https://doi.org/10.1007/s00170-016-8478-7

Elgomati, H. A., Majlis, B. Y., Hamid, A. M. A., Susthitha, P. M., & Ahmad, I. (2012). Modelling of process parameters for 32nm PMOS transistor using Taguchi method. *Proceedings - 6th Asia International Conference on Mathematical Modelling and Computer Simulation, AMS 2012*, 40–45. https://doi.org/10.1109/AMS.2012.22

Ferreira, J. P. d. L., de Castro, D. S., Moreira, I. D. S., da Silva, W. P., de Figueirêdo, R. M. F., & Queiroz, A. J. d. M. (2020). Convective drying kinetics of osmotically pretreated papaya cubes. *Revista Brasileira de Engenharia Agricola e Ambiental*, *24*(3), 200–208. https://doi.org/10.1590/1807-1929/agriambi.v24n3p200-208

Fertig, W. (2018). *Common Duckweed, Lemna minor*. U.S. Forest Service; U.S. Forest Service. https://aquaplant.tamu.edu/plant-identification/alphabetical-index/duckweed/common-duckweed/

Işik, E., Izli, N., Bayram, G., & Turgut, I. (2011). Drying kinetic and physical properties of green laird lentil (lens culinaris) in microwave drying. *African Journal of Biotechnology*, *10*(19), 3841–3848. https://doi.org/10.4314/ajb.v10i19

Jung, J. R., & Yum, B. J. (2011). Uniformity and signal-to-noise ratio for static and dynamic parameter designs of deposition processes. *International Journal of Advanced Manufacturing Technology*, *54*(5–8), 619–628. https://doi.org/10.1007/s00170-010-2957-z

Liu, X., Zhou, Y., Li, C. Q., Lin, Y., Yang, W., & Zhang, G. (2019). Optimization of a new phase change material integrated photovoltaic/thermal panel with the active cooling technique using taguchi method. *Energies*, *12*(6), 1–22. https://doi.org/10.3390/en12061022

Mirzaee, E., Rafiee, S., Keyhani, A., & Emam-Djomeh, Z. (2009). Determining of moisture diffusivity and activation energy in drying of apricots. *Research in Agricultural Engineering*, *55*(3), 114–120. https://doi.org/10.17221/8/2009-rae

Mohammadi, M., Abadeh, A., Nemati-Farouji, R., & Passandideh-Fard, M. (2019). An optimization of heat transfer of nanofluid flow in a helically coiled pipe using Taguchi method. *Journal of Thermal Analysis and Calorimetry*, *138*(2), 1779–1792. https://doi.org/10.1007/s10973-019-08167-y

Montgomery, D. C. (2008). *Mont*. https://doi.org/10.1002/9783527809080.cataz11063

Murphy, B. L. (2015). Chemical Partitioning and Transport in the Environment. In *Introduction to Environmental Forensics: Third Edition* (pp. 165–197). Elsevier Inc. https://doi.org/10.1016/B978-0-12-404696-2.00007-2

Onwude, D. I., Hashim, N., Janius, R. B., Nawi, N. M., & Abdan, K. (2016). Modeling the Thin-Layer Drying of Fruits and Vegetables: A Review. *Comprehensive Reviews in Food Science and Food Safety*, *15*(3), 599–618. https://doi.org/10.1111/1541-4337.12196

özdemir, M. (2020). Optimization of Spring Back in Air V Bending Processing using Taguchi and RSM Method. *Mechanics*, *26*(1), 73–81. https://doi.org/10.5755/j01.mech.26.1.22831

Rao, R. S., Prakasham, R. S., Prasad, K. K., Rajesham, S., Sarma, P. N., & Rao, L. V. (2004). Xylitol production by Candida sp.: Parameter optimization using Taguchi approach. *Process Biochemistry*, *39*(8), 951–956. https://doi.org/10.1016/S0032-9592(03)00207-3

Robinson, T. J., Borror, C. M., & Myers, R. H. (2004). Robust parameter design: A review. *Quality and Reliability Engineering International*, *20*(1), 81–101.

https://doi.org/10.1002/qre.602

Seader, J. D., & Henley, E. J. (2005). *Separation process principles*. Chichester: John Wiley. https://doi.org/10.5860/choice.36-5112

Shammout, W., & Zakaria, H. (2015). Water lentils (duckweed) in Jordan irrigation ponds as a natural water bioremediation agent and protein source for broilers. *Ecological Engineering*, *83*, 71–77. https://doi.org/10.1016/j.ecoleng.2015.05.041

Tang, J., & Sokhansanj, S. (2007). A MODEL FOR THIN-LAYER DRYING OF LENTILS. *Drying Technology*, *December 2014*, 37–41.

Taşkin, O., & İzlı, N. (2019). Effect of microwave, infrared and freeze drying methods on drying kinetics, effective moisture diffusivity and color properties of turmeric. *Tarim Bilimleri Dergisi*, *25*(3), 334–345. https://doi.org/10.15832/ankutbd.439434

Tun, M. M., & Juchelková, D. (2019). Drying methods for municipal solid waste quality improvement in the developed and developing countries: A review. *Environmental Engineering Research*, *24*(4), 529–542. https://doi.org/10.4491/eer.2018.327

		300	400	700	800	1000	2000	4000
Isik et al, 2011	a	1.035	1.0253	1.0285	1.03705			
	b	-1.69E-03	-2.79E-03	-9.11E-02	-9.36E-02			
	c	-0.00041	-0.0005	-0.00056	-0.007			
This paper	a					0.000037	0.000201	0.00007
	b					-0.0114	-0.0339	-0.0168
	c					0.8122	1.6619	0.8686